G3, 2021, 11(8), jkab156
DOI: 10.1093/g3journal/jkab156
Advance Access Publication Date: 6 May 2021
Investigation

Genome-wide screening of genes associated with momilactone B sensitivity in the fission yeast *Schizosaccharomyces pombe*

Keisuke Tomita ,[1] Yoko Yashiroda,[2,*] Yasuhiro Matsuo ,[3] Jeff S. Piotrowski,[2] Sheena C. Li,[2] Reika Okamoto,[2] Mami Yoshimura,[2] Hiromi Kimura,[2] Yumi Kawamura,[2] Makoto Kawamukai,[3] Charles Boone ,[2] Minoru Yoshida,[2,4,5] Hideaki Nojiri,[1,5] and Kazunori Okada[1,*]

[1]Agro-Biotechnology Research Center, Graduate School of Agricultural and Life Sciences, The University of Tokyo, Tokyo 113-8657, Japan
[2]RIKEN Center for Sustainable Resource Science, Wako, Saitama 351-0198, Japan
[3]Institute of Agricultural and Life Sciences, Academic Assembly, Shimane University, Matsue, Shimane 690-8504, Japan
[4]Department of Biotechnology, Graduate School of Agricultural and Life Sciences, The University of Tokyo, Tokyo 113-8657, Japan
[5]Collaborative Research Institute for Innovative Microbiology, The University of Tokyo, Bunkyo-ku, Tokyo 113-8657, Japan

*Corresponding author: RIKEN Center for Sustainable Resource Science, 2-1 Hirosawa, Wako, Saitama 351-0198, Japan; ytyy@riken.jp (Y.Y.); and Agro-Biotechnology Research Center, Graduate School of Agricultural and Life Sciences, The University of Tokyo, 1-1-1 Yayoi, Bunkyo-ku, Tokyo 113-8657, Japan; kokada@g.ecc.u-tokyo.ac.jp (K.O.)

Abstract

Momilactone B is a natural product with dual biological activities, including antimicrobial and allelopathic properties, and plays a major role in plant chemical defense against competitive plants and pathogens. The pharmacological effects of momilactone B on mammalian cells have also been reported. However, little is known about the molecular and cellular mechanisms underlying its broad bioactivity. In this study, the genetic determinants of momilactone B sensitivity in yeast were explored to gain insight into its mode of action. We screened fission yeast mutants resistant to momilactone B from a pooled culture containing genome-wide gene-overexpressing strains in a drug-hypersensitive genetic background. Overexpression of *pmd1*, *bfr1*, *pap1*, *arp9*, or *SPAC9E9.06c* conferred resistance to momilactone B. In addition, a drug-hypersensitive, barcoded deletion library was newly constructed and the genes that imparted altered sensitivity to momilactone B upon deletion were identified. Gene Ontology and fission yeast phenotype ontology enrichment analyses predicted the biological pathways related to the mode of action of momilactone B. The validation of predictions revealed that momilactone B induced abnormal phenotypes such as multiseptated cells and disrupted organization of the microtubule structure. This is the first investigation of the mechanism underlying the antifungal activity of momilactone B against yeast. The results and datasets obtained in this study narrow the possible targets of momilactone B and facilitate further studies regarding its mode of action.

Keywords: phytoalexin; mode of action; septum formation; microtubule; protein quality control; chromatin remodeling

Introduction

Momilactone B, originally isolated from the hull of rice (*Oryza sativa*) (Kato *et al.* 1973), is produced by some species of the genus *Oryza* and the moss *Calohypnum plumiforme* (formerly *Hypnum plumaeforme*) (Nozaki *et al.* 2007; Miyamoto *et al.* 2016). It is known as an allelopathic and antimicrobial agent and has the potential to inhibit the growth of other plants and microorganisms, thus serving as a chemical defense agent against pathogens and competitive plants (Kato-Noguchi *et al.* 2010; Toyomasu *et al.* 2014; Okada *et al.* 2016). Momilactone B inhibits the growth of *Magnaporthe oryzae*, the causative agent of rice blast—one of the most serious fungal diseases worldwide (Cartwright *et al.* 1977). In addition to its intrinsic ecological roles, momilactone B has been reported to exhibit unique functions against mammalian cells, including antitumor, anti-ketotic, and anti-melanogenic properties (Kim *et al.* 2007; Lee *et al.* 2012; Kang *et al.* 2016). These beneficial activities of momilactone B have attracted attention of researchers to exploit this molecule as an herbicide, antimicrobial agent, and pharmaceutical product (Zhao *et al.* 2018). However, little is known about the actual mechanisms underlying its bioactivity, especially at the cellular and molecular levels.

Two yeast species, the budding yeast *Saccharomyces cerevisiae* and the fission yeast *Schizosaccharomyces pombe*, have many favorable features applicable for the identification of targets for bioactive compounds. Notably, there are well-developed collections of deletion and overexpression strains available for these two yeast species (Giaever *et al.* 2002; Sopko *et al.* 2006; Matsuyama *et al.* 2006; Kim *et al.* 2010). These tools allow a comparative analysis of chemical–genetic interactions to provide reliable information about the mode of action of bioactive compounds (Butcher *et al.* 2006; Ho *et al.* 2009; Arita *et al.* 2011; Piotrowski *et al.* 2017). To identify the cellular target of small molecules, drug-hypersensitive

Received: March 12, 2021. **Accepted:** April 28, 2021

fission yeast strains are advantageous because they require only a relatively small amount of the test compound. Membrane transporters, including ATP-binding cassette (ABC) transporters and major facilitator superfamily transporters, have been shown to be involved in the transport of xenobiotics (Lage 2003). Among the 11 ABC transporters in *S. pombe*, Bfr1 or Pmd1 are known to be non-essential for viability and a *bfr1 pmd1* double-deletion strain was shown to be dramatically more sensitive to a wide variety of drugs (Arita *et al.* 2011). Therefore, this strain is feasible for screening for the targets of bioactive compounds, especially rare natural products.

Here, we screened for genes that upon overexpression or deletion confer altered sensitivity to momilactone B in drug-hypersensitive fission yeast, which showed higher sensitivity to momilactone B than budding yeast, to gain insight into the underlying mode of action. From the screening, a list of genetic determinants of momilactone B sensitivity was successfully obtained. Gene Ontology (GO) and fission yeast phenotype ontology (FYPO) enrichment analysis enabled us to predict the cellular processes related to momilactone B. Among them, we validated that momilactone B perturbed proper formation of the septum and the microtubule cytoskeleton.

Materials and methods

Yeast strains and media

S. cerevisiae and *S. pombe* strains used in this study are listed in Table 1. *S. cerevisiae* cultures were grown in YPD medium (2% glucose, 2% Bacto™ peptone, and 1% yeast extract). *S. pombe* cultures were grown in YE medium (0.5% yeast extract, 3% glucose) or YES medium (0.5% yeast extract, 3% glucose, 225 mg/L of adenine, histidine, leucine, lysine, and uracil). Edinburgh minimal medium (EMM, Forsburg and Rhind 2006), which does not contain thiamine, was used to induce gene expression driven by the thiamine-repressible *nmt1* promoter. Adenine, leucine, and uracil were added to the medium if needed. Solid media were prepared using 2% purified agar powder (Nacalai Tesque, Kyoto, Japan) for plate cultures.

Extraction and purification of momilactone B

Rice husks were extracted twice with methanol for 1 day at room temperature. The methanolic extract was filtered through a filter paper and evaporated. The resulting oily residue was suspended in water and extracted with ethyl acetate. The ethyl acetate extract was washed with a saturated solution of sodium chloride (NaCl) and dried *in vacuo* to yield a residue. The residue was separated by several rounds of column chromatography on a silica gel (63–210 mesh, Wakogel 60N; FUJIFILM Wako Pure Chemical, Osaka, Japan) with an elution of ethyl acetate/*n*-hexane or dichloromethane/ethyl acetate. Fractions containing momilactone B were identified using liquid chromatography coupled with electrospray ionization tandem mass spectrometry as previously described (Shimizu *et al.* 2008). Momilactone B-containing fractions were combined and dried *in vacuo*. The residue was dissolved in acetonitrile and purified using high-pressure liquid chromatography on an octadecyl silyl (ODS) column (10 mm i.d. × 25 cm, PEGASIL ODS; Senshu Scientific, Tokyo, Japan) and eluted at a flow rate of 3 mL/min in 70% aqueous acetonitrile. The ^{13}C nuclear magnetic resonance (NMR) spectrum of the compound ($CDCl_3$) showed δ values of 180.45, 148.81, 146.68, 113.99, 110.22, 96.58, 73.73, 72.71, 50.32, 47.40, 44.68, 42.96, 39.98, 37.21, 30.73, 28.80, 26.42, 24.78, 21.85, and 18.98. Momilactone A was purified following the procedure described above. The ^{13}C NMR spectrum ($CDCl_3$) showed δ values of 205.14, 174.28, 148.94, 148.00, 114.04, 110.17, 73.15, 53.56, 50.18, 47.52, 46.47, 40.12, 37.23, 34.87, 32.45, 31.22, 23.99, 21.95, 21.79, and 21.46. Based on comparison with previous literature (Kato *et al.* 1973), the two compounds were confirmed to be momilactone A and B.

Momilactone sensitivity test

Log-phase yeast cells were subjected to a sensitivity test. In the liquid culture test, cells were diluted in fresh medium to obtain an optical density at 600 nm (OD_{600}) of 0.01. The cells were then cultured in the presence of momilactone B at 30°C for 18 h (YES or YPD medium) or 24 h (EMM medium). After incubation, the OD_{600} was measured using an EnSpire™ Multimode Plate Reader (PerkinElmer, Waltham, MA, USA). Momilactone sensitivity was evaluated by growth (%), which was calculated by dividing the OD_{600} measured after growth with momilactone treatment by the OD_{600} measured after growth without momilactone treatment and multiplying by 100. The median effective dose (ED_{50}) of momilactones was calculated using ED50 Calculator (AAT Bioquest, Inc.). In the plate culture test, log-phase inoculum of the cells was diluted to the cell density of 10^7 cells/mL and serially diluted by 10-fold. Aliquots of each dilution were spotted onto agar plates with or without momilactone B. The plates were photographed after incubation for 4 days at 30°C.

Screening for genes that upon overexpression confer resistance to momilactone B

To screen for momilactone B-resistant strains, the glycerol stock of pooled cultures of the drug-hypersensitive strain *bfr1*Δ *pmd1*Δ (YA8) expressing the ORFeome was diluted in EMM liquid medium and incubated for 15 h to induce the expression of the inserted gene under the *nmt1* promoter. The cells were transferred to an EMM agar plate containing 1 μM momilactone B and incubated for 4 days at 30°C. Each ORF insert present in the momilactone B-resistant colonies was amplified by polymerase chain

Table 1 Strains used in this study

Strain	Genotype	Source or reference
S. pombe		
L972	*h*$^-$	Lab stock
JY265	*h*$^-$ *leu1-32*	Arita *et al.* (2011)
YA6	*h*$^-$ *leu1-32 ura4-D18 bfr1::ura4*$^+$	Arita *et al.* (2011)
YA8	*h*$^-$ *leu1-32 ura4-D18 pmd1::hisG bfr1::ura4*$^+$	Arita *et al.* (2011)
YA9	*h*$^-$ *leu1*$^+$*≪pDUAL-FFH1 ura4-D18 pmd1::hisG bfr1::ura4*$^+$	Arita *et al.* (2011)
YY576	*h*$^-$ *mat1≪natMX leu1-32 ura4-D18 pmd1::hph bfr1::ura4*$^+$	This study
YMP384	*h*$^-$ *leu1-32 ura4-D18 kanMX6-nmt1-GFP-atb2 hht1-mRFP-natMX6*	Lab stock
MBY6844	*h*$^-$ *pAct1-Lifeact-mCherry::leu1*$^+$ *ade6-M216 leu1-32 ura4-D18*	Huang *et al.* (2012)
S. cerevisiae		
BY4742	*MATα his3Δ1 leu2Δ0 lys2Δ0 ura3Δ0*	Lab stock

reaction (PCR) using genomic DNA as the template or by direct colony PCR. Genomic DNA was extracted as previously described (Arita *et al.* 2011). The sequences of the common forward and reverse primers were 5-GGGGACAAGTTTGTACAAAAAAGCAGGCT-3′ and 5-CGTCTACATCCTCATCGTTATCGAC-3′, respectively. The DNA polymerase KOD FX Neo (Toyobo, Osaka, Japan) was used for amplification. PCR products were purified and sequenced using the primers described above. In the course of identifying genes overexpressed in momilactone B-resistant strains, most of them were found to be *caf5* or *pmd1* overexpression strains. To identify colonies overexpressing these two genes, the PCR products were blotted onto a Biodyne B nylon membrane (Pall Corp., Port Washington, NY, USA) and subjected to Southern hybridization analysis using *caf5* and *pmd1* probes labeled with digoxigenin (DIG). To prepare *caf5* and *pmd1* probes, the partial fragment of each gene was PCR-amplified using the genomic DNA of YA8 as the template and the following primer pairs: 5-AAACCGTTTTCGGCGAATTG-3′ and 5-CGGCTTCTCAG TTTCAGACC-3′ for *caf5* and 5-CTGAACGTTGCTTCGCTGAG-3′ and 5-AATGATGCGATTGCCGACTC-3′ for *pmd1*. The DNA was labeled with DIG-High Prime (Roche Applied Science, Mannheim, Germany), and DIG-labeled DNA was detected using anti-DIG-AP, Fab fragments, and NBT/BCIP (Roche Applied Science).

Genome-wide fitness profiling using a gene deletion library

A high-throughput chemical-genetic screening platform for *S. pombe* was constructed based on a similar platform developed for *S. cerevisiae* (Piotrowski *et al.* 2017). A hypersensitive, barcoded h^- deletion mutant library was prepared as follows. To construct the drug-sensitive h^- query strain (YY576), YA6 (Arita *et al.* 2011) was used as the host. The $pmd1^+$ gene of YA6 was disrupted by replacement with the hygromycin-resistant *hph* gene. The *natMX* marker that provides resistance to the drug nourseothricin (NAT) was inserted adjacent to the *mat1* locus. YY576 was crossed with the Bioneer barcoded h^+ deletion library (version 1.0) and sporulated on EMM + Ade + Ura + Leu. The resultant spores were transferred to EMM + Leu and then to YE containing G418, hygromycin, and NAT to select for the h^- *pmd1*Δ *bfr1*Δ *xxx*Δ meiotic progeny. Our genome-wide drug-sensitive fission yeast deletion collection contained 2,195 strains (Supplementary Table 1). The pool of deletion mutants was created as previously described (Piotrowski *et al.* 2017). The final concentration of the pool was adjusted to 32 OD_{600}/mL in YE + Ade + Ura + Leu media containing 15% glycerol, and the stocks were stored at −80°C until required. Cells were thawed and diluted 1:100 (~150 cells/strain) in 200 µL of YE in a 96-well flat-bottom plate. Cultures were spiked with different concentrations (0.6, 0.7, and 0.8 µM) of momilactone B ($n = 2$ for each concentration) or a 1% dimethyl sulfoxide control ($n = 4$) and grown for 48 h at 30°C. Genomic DNA was purified from harvested cells; PCR amplification of UPTAG barcodes using the multiplex primers and gel purification of barcodes were carried out as previously described (Piotrowski *et al.* 2017). The barcodes from each sample were sequenced on an Illumina MiSeq using MiSeq Reagent Kit v3 (150 cycles) (Illumina Inc., San Diego, CA, USA). The barcode counts for each deletion mutant were quantified using BEAN-counter software to generate chemical genetic interaction scores (Simpkins *et al.* 2019). Regarding the deletion mutants of 6 genes (*SPCC1827.07c*, *phb2*, *vps16*, *SPAC1A6.01c*, *gcn20*, and *vms1*), whose sensitivity to momilactone B was individually tested, proper integration of KanMX cassettes was confirmed by PCR and G418 resistance. Gene and phenotype ontology enrichment analyses were performed using the AnGeLi web tool (Bitton *et al.* 2015). *P*-values were adjusted based on false discovery rate. Enrichment analysis was conducted by comparing the gene mutants that confer resistance or hypersensitivity to momilactone B with the background distribution of gene mutants for which the Z-score can be calculated in all experiments.

Microscopic observation

Log-phase cells were diluted in fresh medium to an OD_{600} of 0.1 and then incubated at 30°C with or without 10 µM momilactone B. For septum staining, the cultured cells were treated with glutaraldehyde (25% in water) at a final concentration of 10% (v/v) for 30 min at 4°C. The fixed cells were washed three times with phosphate-buffered saline (PBS). The PBS-suspended cells were mixed with the same volume of calcofluor white stain (Sigma Aldrich, St. Louis, MO, USA) and observed under a microscope BX51 (Olympus, Tokyo, Japan) or BZ-X800 (Keyence, Osaka, Japan).

Results and discussion

Momilactone B inhibits the growth of S. cerevisiae and S. pombe at micromolar concentrations

The growth-inhibitory effect of momilactone B, which structurally belongs to a pimerane-type diterpene bearing a 9β-H (Figure 1), has been reported in some species of phytopathogenic fungi (Fukuta *et al.* 2007). However, the fungicidal activity of momilactone B toward the two yeast species, *S. cerevisiae* and *S. pombe*, has not been investigated. Therefore, we first tested the effects of momilactone B on the growth of these two yeasts. To assess the sensitivity of the yeast cells to momilactone B, liquid cultures of log-phase yeast cells containing various concentrations of momilactone B were incubated and cell growth was assessed by measuring the culture density (OD_{600}). Dose–responses and ED_{50} values calculated from them showed that *S. pombe* was more sensitive to momilactone B than *S. cerevisiae* (Supplementary Figure 1 and Table 2). We also tested the inhibitory effect of the other structurally related momilactone isoform, momilactone A (Figure 1). Although the anti-proliferative activity of momilactone A was weaker than that of momilactone B, momilactone A also inhibited the growth of both yeast cells. This observation is consistent with a previous report, wherein momilactone B exerted more potent herbicidal and fungicidal activities than momilactone A (Fukuta *et al.* 2007; Kato-Noguchi and Ota 2013). Therefore, we decided to use *S. pombe* for the remainder of this study.

Identification of genes that upon overexpression confer resistance to momilactone B

As the mechanism underlying the antifungal activity of momilactones has not been investigated, we adopted a genome-wide approach to comprehensively identify the genes related to momilactone B sensitivity. A collection of ~5,000 different fission yeast ORFeome-expressing strains was previously constructed using a drug-hypersensitive strain lacking two genes encoding drug efflux pumps *bfr1* and *pmd1* as a background host (Arita *et al.* 2011). As shown in Figure 2A, deletion of these two genes rendered the fission yeast cells more sensitive to momilactone B. The experimental procedure for screening is outlined in Figure 2B. Pooled cultures of the ORFeome-expressing strains were incubated on EMM agar plates containing 1 µM momilactone B, and a total of 679 resistant colonies were obtained by screening about 2,500,000 cells. As shown in Table 3, five ORFs were integrated into the resistant colonies. To confirm the results of the screening, we evaluated the momilactone B sensitivity of the resistant strains identified. All the ORFs were validated to confer visible resistance to momilactone B upon overexpression to varying degrees on a solid medium

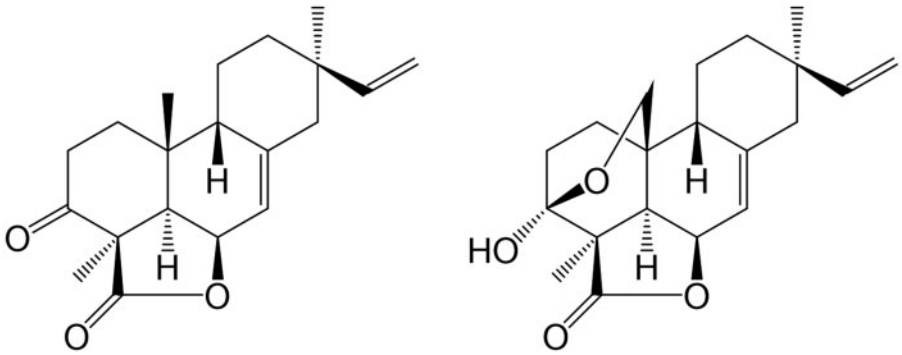

Figure 1 The chemical structures of momilactone A (left) and momilactone B (right).

Table 2 ED_{50} values (μM) of momilactones against two yeast species

	S. cerevisiae BY4742	*S. pombe* L972
Momilactone A	>40	3.52
Momilactone B	14.3	1.27

(Figure 2C). Although the resistance to momilactone B of *arp9*-overexpressing strain was difficult to evaluate on the solid medium, we were able to observe the statistically significant momilactone B resistance of the *arp9*-overexpressing strain in the liquid culture (Supplementary Figure 2).

Caf5 and Pmd1 are transporters that are known to provide resistance against a wide range of drugs (Arita *et al.* 2011; Kawashima *et al.* 2012). As the strain used in the screening was defective in *pmd1* and hypersensitive to momilactone B, it seems reasonable that the overexpression of *pmd1* may decrease drug sensitivity. Caf5 has been reported to endow fission yeast cells with caffeine resistance, probably through the efflux of caffeine (Benko *et al.* 2004; Calvo *et al.* 2009). Our results suggest that Caf5 can transport not only alkaloids such as caffeine but also diterpenoid compounds. Pap1 is known to be a key transcription factor that responds to drug stress and induces the expression of drug-resistant transporters, including *caf5* and *pmd1* (Toone *et al.* 1998; Kawashima *et al.* 2012; Asadi *et al.* 2017). A possible reason for momilactone B resistance in *pap1*-overexpressing cells could be the enhanced transcription of transporter genes such as *caf5*.

In the screening, we also found that the overexpression of either *arp9* or *SPAC9E9.06c* resulted in a slight increase in the resistance of fission yeast to momilactone B. *arp9* is a non-essential gene homolog encoding nuclear actin-related proteins, which are important components of the SWI/SNF and RSC chromatin remodeling and modifying complexes (Monahan *et al.* 2008). It has been reported that *arp9* deletion mutant was hypersensitive to drugs (Monahan *et al.* 2008), suggesting that Arp9 is involved in drug resistance or momilactone B may affect its functionality as a cofactor of chromatin remodeling complexes or another unknown mechanism. *SPAC9E9.06c* is predicted to encode a threonine synthase and is essential for vegetative growth (Kim *et al.* 2010; Hayles *et al.* 2013). Although there is no experimental evidence of the enzymatic function of this gene, it may serve as a candidate target of momilactone B in fission yeast.

Identification of genes that upon deletion alter the sensitivity to momilactone B

To gain a more informative and global scenario of the mode of action of momilactone B, we performed a genome-wide fitness profiling to identify genes that upon deletion alter the sensitivity to momilactone B. The resulting set of sensitive and resistant gene-deletion mutants might provide an insight into the mode of action of momilactone B.

A genome-wide collection of drug-hypersensitive deletion strains was prepared using a strain deficient in *bfr1* and *pmd1*, as well as the ORFeome-expressing strains used above (Arita *et al.* 2011). Drug-hypersensitive deletion strains were constructed by crossing the disruptant of *bfr1* and *pmd1* with a previously constructed gene-deletion library (Kim *et al.* 2010). A total of 2,195 strains were constructed by incorporating a strain-specific barcode sequence into the genome along with the deletion cassette (Supplementary Table 1). The barcodes enabled us to distinguish the genomic DNA of one deletion strain from that of another and measure the global fitness of deletion mutants in one pooled culture.

A schematic representation of the screening process is presented in Figure 3A. A pooled mixture of the newly constructed deletion mutants was incubated with or without momilactone B. The genomic DNA was subsequently extracted from the culture, and the strain-specific DNA barcode regions were PCR-amplified followed by sequencing. The Z-scores were calculated to measure the relative fitness of each strain treated with momilactone B to the control (Figure 3B). A negative Z-score represents hypersensitivity to momilactone B, whereas a positive Z-score represents resistance. We repeated the experiment twice as a biological replication; in each experiment, the pooled culture was treated with momilactone B at concentrations of 0.6, 0.7, and 0.8 μM. The Z-scores of each gene deletion mutant are listed in Supplementary Table 2. The Z-scores were successfully calculated for 1,664 of 2,195 genes (75.8%) in all samples. We set a Z-score threshold of ±2, and deletion mutants satisfying this criterion in both biological replicates were defined as resistant or hypersensitive. As a result, 13–40 deletion mutants were identified as hypersensitive to momilactone B (Supplementary Table 3) and 31–79 gene-deletion mutants were identified as resistant to momilactone B (Supplementary Table 4) depending on the concentration of momilactone B. The number of resistant/hypersensitive strains increased with the increase of momilactone B concentration. Furthermore, most of the resistant/hypersensitive strains at lower doses were included in those at higher doses (Figures 3, C and D). These results suggested that the overall Z-scores showed more characteristic pattern to the compound at higher doses. To confirm the calculated Z-scores reflected the momilactone B sensitivity, three of each resistant or hypersensitive deletion mutants were selected and subjected to the individual test for momilactone B sensitivity. As shown in Figure 3E, all of them showed resistance or hypersensitivity to momilactone B.

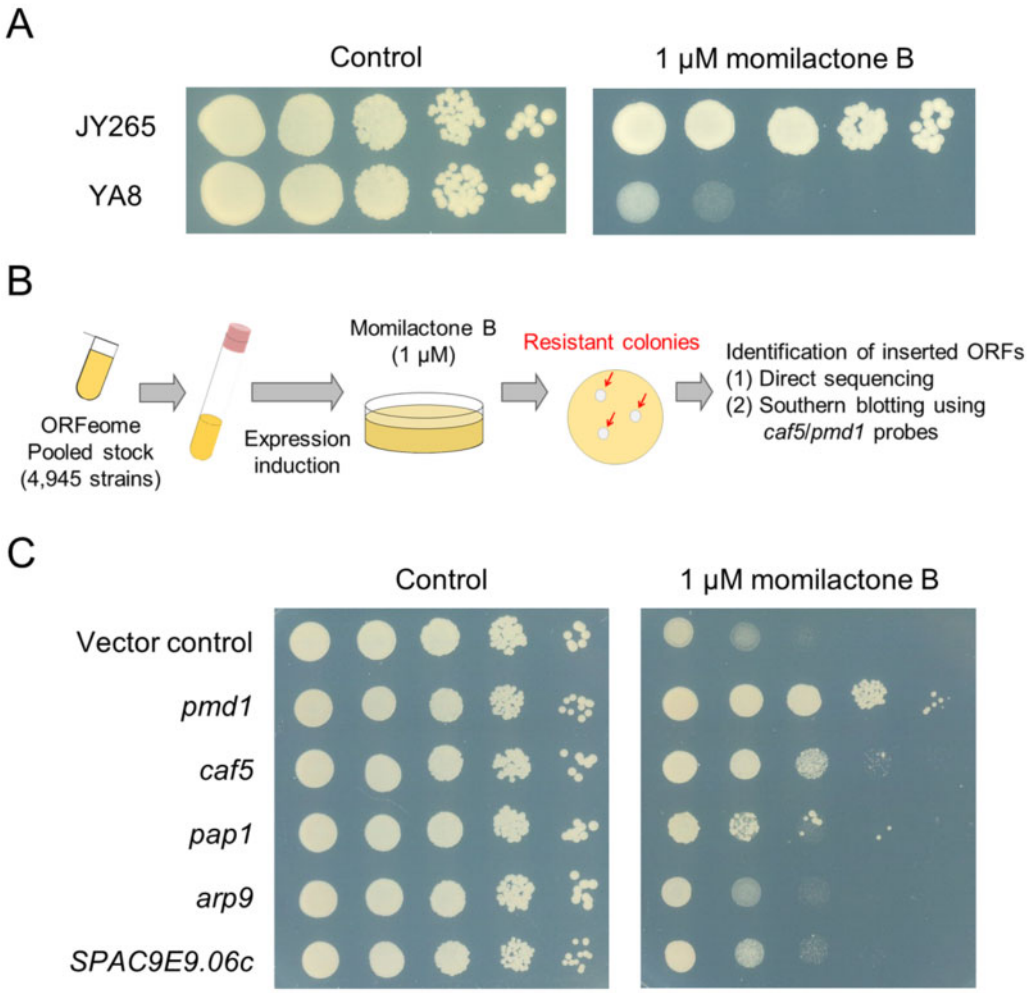

Figure 2 Genome-wide screening for multicopy suppressors of momilactone B cytotoxicity. (A) Anti-proliferative activity of momilactone B against the drug-hypersensitive fission yeast. Log-phase cultures of JY265 (parental strain) and YA8 (drug-hypersensitive) were adjusted to the cell density of 10^7 cells/mL and serially diluted by 10-fold. Aliquots of each dilution were spotted onto YES agar plates containing 1 μM of momilactone B and incubated for 4 days at 30°C. (B) Schematic representation of the screening procedure. A pooled culture containing fission yeast strains overexpressing a different ORF was spread onto EMM agar plates containing 1 μM momilactone B. After the incubation, growing colonies were picked up and the inserted ORFs were identified. (C) Validation of the results from the screening. Log-phase inoculum of the resistant strains in the drug-hypersensitive genetic background identified in the screen and the vector control YA9 were diluted to the cell density of 10^7 cells/mL and serially diluted by 10-fold. Aliquots of each dilution were spotted onto EMM agar plates with or without 1 μM momilactone B and incubated for 4 days at 30°C.

Table 3 Inserted ORFs into momilactone B-resistant colonies

Gene name	Product[a]	Colony number
pmd1	Leptomycin transmembrane transporter	403
caf5	Spermine family transmembrane transporter	243
pap1	AP-1 like transcription factor	31
arp9	SWI/SNF and RSC complex subunit	1
SPAC9E9.06c	Threonine synthase (predicted)	1

[a]These descriptions are from Pombase (https://www.pombase.org/).

GO enrichment analysis

Next, we used the web-tool AnGeLi (Bitton *et al.* 2015) to detect the GO and FYPO terms enriched in the list of the genes that upon deletion conferred altered momilactone B sensitivity.

The sensitized genes were enriched in GO and FYPO terms, especially gene expression, cellular metabolic processes, and cellular protein levels, suggesting that momilactone B perturbs diverse and fundamental biological processes (Supplementary Table 5). In addition, the FYPO terms related to defects in septum formation, such as premature septum assembly and abnormal septum assembly, were enriched. The FYPO term of altered sensitivity to thiabendazole, an inhibitor of microtubule polymerization, was also enriched. These results raise the possibility that momilactone B perturbs septum formation and microtubule function.

To verify this hypothesis, the effect of momilactone B on septum formation and microtubule structure of fission yeast was examined. Interestingly, fission yeast cells of the wild-type L972 treated with momilactone B showed abnormal morphology such as branched, elongated, and multiseptate cells with branch forming adjacent to septum (Figure 4A). It was previously

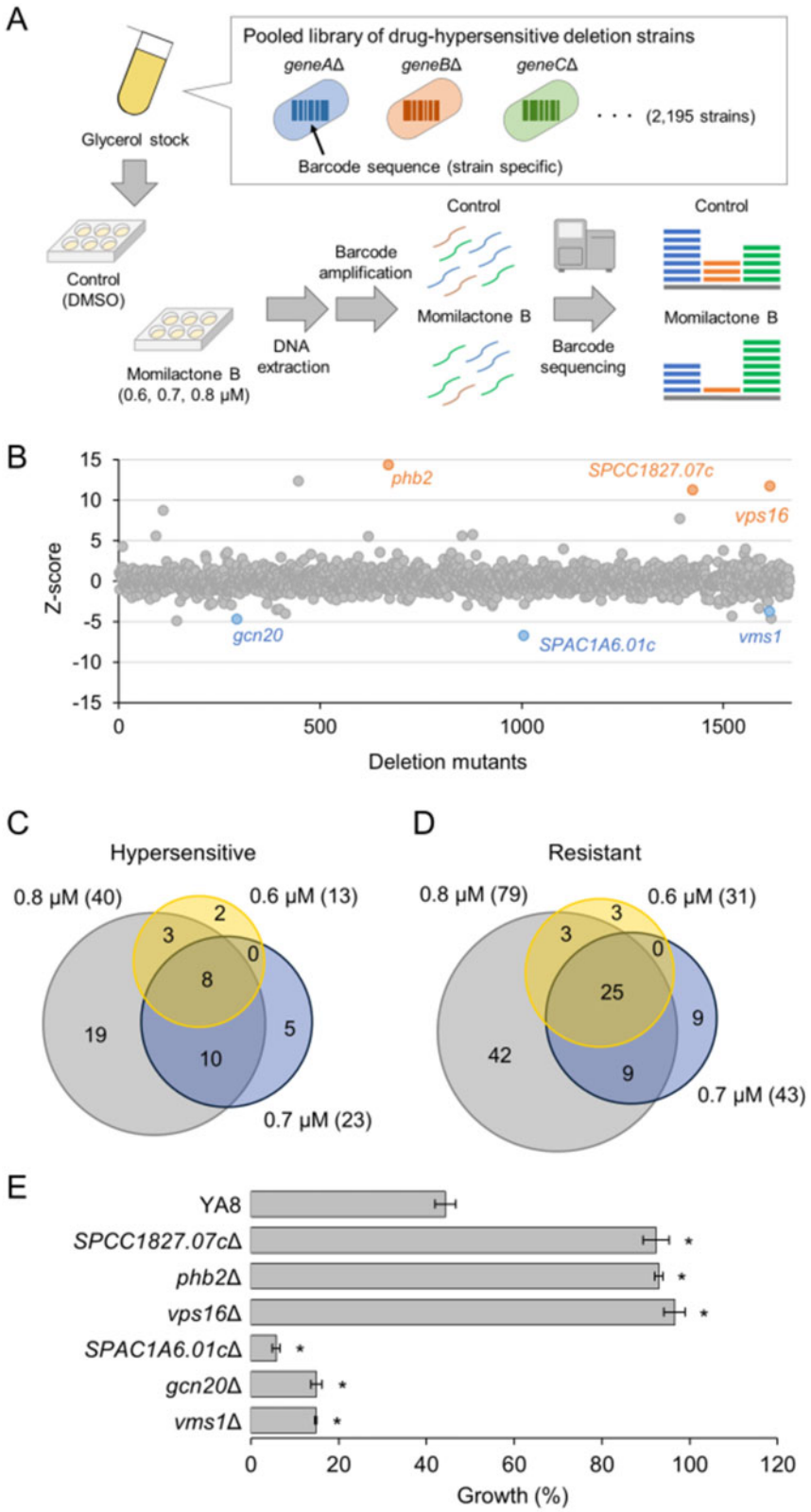

Figure 3 Genome-wide screening for identifying deletion mutants hypersensitive or resistant to momilactone B. (A) Schematic representation of the screening process. A pooled culture containing 2,195 fission yeast deletion mutants in the drug-hypersensitive genetic background was incubated with or without momilactone B. Subsequently, the genomic DNA was extracted from the culture and the inserted barcode regions were PCR amplified and sequenced. Finally, to measure the relative fitness of each strain, Z-scores were calculated by comparing the read counts from the momilactone B treatment sample to the control. (B) Overall Z-scores from the genome-wide screen. Z-scores from the experiment (0.7 μM momilactone B, #2) were shown as a representative dataset. (C and D) Venn diagrams showing the overlap of deletion mutants identified as hypersensitive (C) or resistant (D) to momilactone B. The total number of genes that upon deletion altered the sensitivity to momilactone B at each dose is indicated in parentheses. (E) Validation of the results from the screening. Log-phase inoculums of the deletion strains of top-hit genes in the drug-hypersensitive genetic background were diluted to an OD_{600} of 0.01 and exposed to 0.3 μM momilactone B in YES liquid medium for 18 h at 30°C. Bars indicate the growth of momilactone B-treated cells, which is normalized relative to the growth of untreated cells ($n = 3$, mean ± SD). Asterisks indicate significant differences relative to the wild type assessed by Welch's *t*-test (*$P < 0.01$).

demonstrated that momilactone B had inhibitory effects on alpha-amylase and alpha-glucosidase (Quan *et al.* 2019). It is conceivable that momilactone B may inhibit cell separation by disturbing activities of the related enzymes such as polysaccharide degrading enzymes Agn1 or Eng1, which are required for proper cell separation (Sipiczki 2007). Microscopic observation of the cells of YMP384 expressing RFP-tagged Hht1 (histone H3) and GFP-tagged Atb2 (tubulin alpha 2) revealed that the cells with multiple septa mediated by momilactone B treatment had nuclei in each cell separated by septa. Some abnormally shaped cells showed curved microtubules at their tips, which were not observed in the control (Figure 4B). As abnormal cell morphology was mediated by momilactone B treatment, the effect of momilactone B on the localization of actin, another major factor regulating cell shape, was investigated. As shown in Supplementary Figure 3, no apparent changes were found. Taken together, these data indicate that momilactone B affects septum formation and microtubule structure of fission yeast, consistent with the prediction from the genome-wide fitness profiling of deletion mutants.

Furthermore, in association with the fact that *arp9* overexpressing strain showed resistance to momilactone B (Figure 2C and Supplementary Figure 2), gene ontologies related to chromatin remodeling were enriched in the sensitized genes, indicating that chromatin remodeling plays a role in determining momilactone B sensitivity. In the sensitized genes, we found the components of Set1 complex (*swd1*, *swd3*, and *spf1*) and Lem2-Nur1 complex (*lem2* and *nur1*), both of which catalyze methylation of histone H3 (Roguev *et al.* 2003; Banday *et al.* 2016). Considering that disruption of the components of these complexes caused hypersensitivity to thiabendazole (Pan *et al.* 2012; Banday *et al.* 2016), hypersensitivity to momilactone B of these deletion mutants may be because momilactone B disrupts microtubule structure (Figure 4B).

Among the resistant genes, those involved in cytoplasmic translation, such as the subunit of the cytosolic ribosome, were

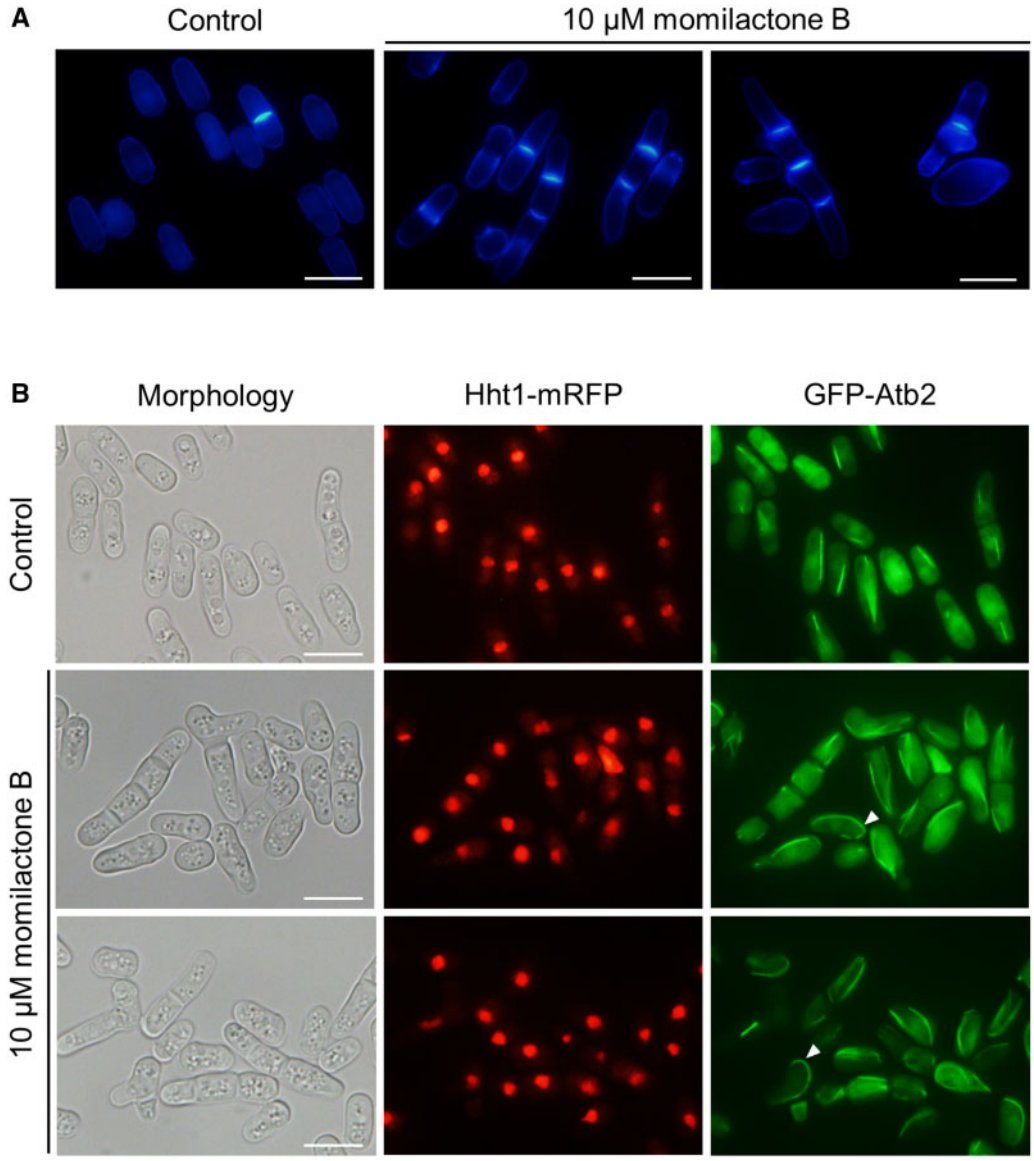

Figure 4 Abnormal septum and microtubule formation of *S. pombe* cells after treated with momilactone B. (A) Wild-type strain L972 was incubated for 24 h at 30°C with 10 μM momilactone B. Cells were fixed and stained with calcofluor white. (B) YMP384 strain expressing Hht1-mRFP and GFP-Atb2 was incubated for 24 h at 30°C with 10 μM momilactone B. Histone and microtubules were observed using fluorescent microscopy after incubation. Scale bar: 10 μm. Arrowheads indicate curved microtubules.

enriched. Thus, translation is a candidate biological process targeted by momilactone B (Supplementary Table 6). Interestingly, the deletion mutants of the genes involved in ribosome-associated quality control (RQC) in their budding yeast orthologs, *SPAC1A6.01c* and *vms1* (Izawa *et al.* 2017; Matsuo *et al.* 2017; Su *et al.* 2019), were found to be hypersensitive to momilactone B (Figure 3E and Supplementary Table 3). One possible explanation for this phenomenon is that momilactone B inhibits the translation of fission yeast cells and induces the production of aberrant proteins, which is normally suppressed by the action of RQC to maintain the quality of translated proteins. Once RQC is disabled, the aberrant protein production in the ribosomal unit appears to have a greater impact on cell growth retardation. Thus, the RQC-defective mutant becomes hypersensitive to momilactone B, which might act as a translation inhibitor. Consistently, some deletion mutants of genes required for the onset of RQC were hypersensitive to the translation inhibitor anisomycin (Matsuo *et al.* 2017). In addition, deletion mutants of ribosomal units were less sensitive to momilactone B treatment, probably owing to their reduced activity for translation, and thus had reduced risk of toxic aberrant protein production.

A number of natural products with unique and potent bioactivity have been isolated. However, their biological modes of action remain to be elucidated. In this study, we first identified the genetic determinants of momilactone B sensitivity to predict the mode of action of this plant-derived natural product. By confirming the hypothesis predicted from genome-wide screening, we demonstrated that momilactone B perturbs the proper organization of microtubule structure and septum formation. Demonstrating the involvement of other candidate targets in the mode of action of momilactone B will be a future challenge. In addition, we constructed a new drug-hypersensitive, barcoded gene deletion library of the fission yeast. This library will facilitate target identification of bioactive compounds, especially valuable natural products such as momilactone B.

Data availability

The data underlying this article are available in the article and in its Supplementary Material.

Acknowledgments

We are grateful to Dr. Morifumi Hasegawa for technical support in the purification of momilactones, Dr. Kenji Tomita for assistance with NMR analysis, and Dr. Mohan K. Balasubramanian, Dr. Akihisa Matsuyama, and Mr. Atsushi Hashimoto for providing the yeast strains. We also thank Support Unit for Bio-Material Analysis, RIKEN CBS Research Resources Division, for technical help with the MiSeq analysis.

Funding

This study was partially supported by JSPS KAKENHI (grant number 17H03811 and 20H02922 to K.O. and 19H05640 to M.Y.), Japan-Austria Research Cooperative Program between JSPS and FWF (grant number JPJSBP120202002 to K.O.), a JSPS Grant-in-Aid for Scientific Research on Innovative Areas (grant number 17H06411 to C.B. and Y.Y.), a Grant-in-Aid for JSPS Research Fellow (grant number 19J14746 to K.T.), Shorai Foundation for Science and Technology, and NAGASE Science Technology Foundation to K.O. J.S.P., and S.C.L. were supported by a RIKEN Foreign Postdoctoral Research Fellowship.

Conflicts of interest

The authors declare no conflicts of interest associated with this manuscript.

Literature cited

Arita Y, Nishimura S, Matsuyama A, Yashiroda Y, Usui T, *et al.* 2011. Microarray-based target identification using drug hypersensitive fission yeast expressing ORFeome. Mol BioSyst. 7:1463–1472.

Asadi F, Chakraborty B, Karagiannis J. 2017. Latrunculin A-induced perturbation of the actin cytoskeleton mediates Pap1p-dependent induction of the Caf5p efflux pump in *Schizosaccharomyces pombe*. G3 (Bethesda). 7:723–730.

Banday S, Farooq Z, Rashid R, Abdullah E, Altaf M. 2016. Role of inner nuclear membrane protein complex Lem2-Nur1 in heterochromatic gene silencing. J Biol Chem. 291:20021–20029.

Benko Z, Fenyvesvolgyi C, Pesti M, Sipiczki M. 2004. The transcription factor Pap1/Caf3 plays a central role in the determination of caffeine resistance in *Schizosaccharomyces pombe*. Mol Genet Genomics. 271:161–170.

Bitton DA, Schubert F, Dey S, Okoniewski M, Smith GC, *et al.* 2015. AnGeLi: a tool for the analysis of gene lists from fission yeast. Front Genet. 6: 330.

Butcher RA, Bhullar BS, Perlstein EO, Marsischky G, LaBaer J, *et al.* 2006. Microarray-based method for monitoring yeast overexpression strains reveals small-molecule targets in TOR pathway. Nat Chem Biol. 2:103–109.

Calvo IA, Gabrielli N, Iglesias-Baena I, García-Santamarina S, Hoe K-L, *et al.* 2009. Genome-wide screen of genes required for caffeine tolerance in fission yeast. PLoS One. 4:e6619.

Cartwright D, Langcake P, Pryce RJ, Leworthy DP, Ride JP. 1977. Chemical activation of host defence mechanisms as a basis for crop protection. Nature. 267:511–513.

Forsburg SL, Rhind N. 2006. Basic methods for fission yeast. Yeast. 23:173–183.

Fukuta M, Xuan TD, Deba F, Tawata S, Khanh TD, *et al.* 2007. Comparative efficacies in vitro of antibacterial, fungicidal, antioxidant, and herbicidal activities of momilactones A and B. J Plant Interact. 2:245–251.

Giaever G, Chu AM, Ni L, Connelly C, Riles L, *et al.* 2002. Functional profiling of the *Saccharomyces cerevisiae* genome. Nature. 418: 387–391.

Hayles J, Wood V, Jeffery L, Hoe K-L, Kim D-U, *et al.* 2013. A genome-wide resource of cell cycle and cell shape genes of fission yeast. Open Biol. 3:130053.

Ho CH, Magtanong L, Barker SL, Gresham D, Nishimura S, *et al.* 2009. A molecular barcoded yeast ORF library enables mode-of-action analysis of bioactive compounds. Nat Biotechnol. 27:369–377.

Huang J, Huang Y, Yu H, Subramanian D, Padmanabhan A, *et al.* 2012. Nonmedially assembled F-actin cables incorporate into the actomyosin ring in fission yeast. J Cell Biol. 199:831–847.

Izawa T, Park S-H, Zhao L, Hartl FU, Neupert W. 2017. Cytosolic protein Vms1 links ribosome quality control to mitochondrial and cellular homeostasis. Cell. 171:890–903.

Kang D, Nipin S, Darvin P, Joung Y, Byun H, *et al.* 2016. Momilactone B inhibits ketosis in vitro by regulating the ANGPTL3-LPL pathway and inhibiting HMGCS2. Anim Biotechnol. 28:189–197.

Kato T, Kabuto C, Sasaki N, Tsunagawa M, Aizawa H, *et al.* 1973. Momilactones, growth inhibitors from rice. Oryza sativa L. Tetrahedron Lett. 14:3861–3864.

Kato-Noguchi H, Hasegawa M, Ino T, Ota K, Kujime H. 2010. Contribution of momilactone A and B to rice allelopathy. J Plant Physiol. 167:787–791.

Kato-Noguchi H, Ota K. 2013. Biological activities of rice allelochemicals momilactone A and B. J Rice Res. 1:108.

Kawashima SA, Takemoto A, Nurse P, Kapoor TM. 2012. Analyzing fission yeast multidrug resistance mechanisms to develop a genetically tractable model system for chemical biology. Chem Biol. 19:893–901.

Kim D-U, Hayles J, Kim D, Wood V, Park H-O, *et al.* 2010. Analysis of a genome-wide set of gene deletions in the fission yeast *Schizosaccharomyces pombe*. Nat Biotechnol. 28:617–623.

Kim S-J, Park H-R, Park E, Lee S-C. 2007. Cytotoxic and antitumor activity of momilactone B from rice hulls. J Agric Food Chem. 55: 1702–1706.

Lage H. 2003. ABC-transporters: implications on drug resistance from microorganisms to human cancers. Int J Antimicrob Agents. 22:188–199.

Lee J, Cho B, Jun H, Seo W-D, Kim D-W, *et al.* 2012. Momilactone B inhibits protein kinase A signaling and reduces tyrosinase-related proteins 1 and 2 expression in melanocytes. Biotechnol Lett. 34:805–812.

Matsuo Y, Ikeuchi K, Saeki Y, Iwasaki S, Schmidt C, *et al.* 2017. Ubiquitination of stalled ribosome triggers ribosome-associated quality control. Nat Commun. 8:159.

Matsuyama A, Arai R, Yashiroda Y, Shirai A, Kamata A, *et al.* 2006. ORFeome cloning and global analysis of protein localization in the fission yeast *Schizosaccharomyces pombe*. Nat Biotechnol. 24: 841–847.

Miyamoto K, Fujita M, Shenton MR, Akashi S, Sugawara C, *et al.* 2016. Evolutionary trajectory of phytoalexin biosynthetic gene clusters in rice. Plant J. 87:293–304.

Monahan BJ, Villén J, Marguerat S, Bähler J, Gygi SP, *et al.* 2008. Fission yeast SWI/SNF and RSC complexes show compositional and functional differences from budding yeast. Nat Struct Mol Biol. 15:873–880.

Nozaki H, Hayashi K, Nishimura N, Kawaide H, Matsuo A, *et al.* 2007. Momilactone A and B as allelochemicals from moss *Hypnum plumaeforme*: First occurrence in bryophytes. Biosci Biotechnol Biochem. 71:3127–3130.

Okada K, Kawaide H, Miyamoto K, Miyazaki S, Kainuma R, *et al.* 2016. HpDTC1, a stress-inducible bifunctional diterpene cyclase involved in momilactone biosynthesis, functions in chemical defence in the moss *Hypnum plumaeforme*. Sci Rep. 6:25316.

Pan X, Lei B, Zhou N, Feng B, Yao W, *et al.* 2012. Identification of novel genes involved in DNA damage response by screening a genome-wide *Schizosaccharomyces pombe* deletion library. BMC Genomics. 13:662.

Piotrowski JS, Li SC, Deshpande R, Simpkins SW, Nelson J, *et al.* 2017. Functional annotation of chemical libraries across diverse biological processes. Nat Chem Biol. 13:982–993.

Quan NV, Xuan TD, Tran H-D, Ahmad A, Khanh TD, *et al.* 2019. Contribution of momilactones A and B to diabetes inhibitory potential of rice bran: Evidence from in vitro assays. Saudi Pharm J. 27:643–649.

Roguev A, Schaft D, Shevchenko A, Aasland R, Shevchenko A, *et al.* 2003. High conservation of the Set1/Rad6 axis of histone 3 lysine 4 methylation in budding and fission yeasts. J Biol Chem. 278: 8487–8493.

Shimizu T, Jikumaru Y, Okada A, Okada K, Koga J, *et al.* 2008. Effects of a bile acid elicitor, cholic acid, on the biosynthesis of diterpenoid phytoalexins in suspension-cultured rice cells. Phytochem. 69:973–981.

Simpkins SW, Deshpande R, Nelson J, Li SC, Piotrowski JS, *et al.* 2019. Using BEAN-counter to quantify genetic interactions from multiplexed barcode sequencing experiments. Nat Protoc. 14:415–440.

Sipiczki M. 2007. Splitting of the fission yeast septum. FEMS Yeast Res. 7:761–770.

Sopko R, Huang D, Preston N, Chua G, Papp B, *et al.* 2006. Mapping pathways and phenotypes by systematic gene overexpression. Mol Cell. 21:319–330.

Su T, Izawa T, Thoms M, Yamashita Y, Cheng J, *et al.* 2019. Structure and function of Vms1 and Arb1 in RQC and mitochondrial proteome homeostasis. Nature. 570:538–542.

Toone WM, Kuge S, Samuels M, Morgan BA, Toda T, *et al.* 1998. Regulation of the fission yeast transcription factor Pap1 by oxidative stress: requirement for the nuclear export factor Crm1 (Exportin) and the stress-activated MAP kinase Sty1/Spc1. Gene Dev. 12:1453–1463.

Toyomasu T, Usui M, Sugawara C, Otomo K, Hirose Y, *et al.* 2014. Reverse-genetic approach to verify physiological roles of rice phytoalexins: characterization of a knockdown mutant of *OsCPS4* phytoalexin biosynthetic gene in rice. Physiol Plant. 150:55–62.

Zhao M, Cheng J, Guo B, Duan J, Che C-T. 2018. Momilactone and related diterpenoids as potential agricultural chemicals. J Agric Food Chem. 66:7859–7872.

Communicating editor: C. S. Hoffman